INVESTIGATION OF THE MICROSTRUCTURE OF AISI 321 STAINLESS STEEL AFTER LASER SURFACE MELTING

Tsanka D. Dikova[1], Natalina K. Panova[2], Ivaylo D. Parushev[1]

[1]*Faculty of Dental Medicine*
Medical University "Prof. Dr. Paraskev Stoyanov" - Varna
84 Tsar Osvoboditel blvd., Varna 9000, Bulgaria
[2]*Faculty of Pharmacy*
Medical University "Prof. Dr. Paraskev Stoyanov" - Varna
84 Tsar Osvoboditel blvd., Varna 9000, Bulgaria
E-mail: tsanka_dikova@abv.bg

Received 31 July 2023
Accepted 27 September 2023
DOI: 10.59957/jctm.v59.i1.2024.24

ABSTRACT

The aim of the present paper is to investigate the microstructure of laser-melted surface layers of austenitic steel for biomedical applications. The surface of prismatic specimens from AISI 321 stainless steel was treated by continuous CO_2 laser. Three modes of laser processing were used, ensuring surface melting. The microstructure was observed by OM and SEM, while the chemical composition was investigated by EDX analysis. It was found that the microstructure of as-delivered steel was two-phase and relatively inhomogeneous in morphology and chemical composition. It consisted of austenite with grain sizes between 20 - 150 μm, relatively large amount of striped δ-ferrite and spherical carbides along the grain boundaries. After laser melting, the microstructure remained two-phase (δ-ferrite and austenite), but became more homogeneous in morphology and composition. Different dendrites morphology in the particular regions of the molten layer was confirmed - fine equiaxed dendrites on the top surface and columnar at the bottom of the molten pool. Delta-ferrite is located in the interdendritic areas and in larger amounts in the transition zone between the molten layer and the base metal.

Keywords: medical devices, implant materials, austenitic stainless steel, laser surface melting, microstructure.

INTRODUCTION

Austenitic stainless steels are used in medicine for manufacturing various types of non-implantable medical devices, short-term implants and implants in orthopedics [1 - 3]. They are characterized by higher mechanical properties than titanium and Co-Cr alloys, high corrosion resistance and biocompatibility. On the one hand, their high corrosion resistance is due to the monophasic austenite structure, and on the other to the dense layer of chromium oxides that forms on the surface and protects the steel from further interaction with the oxygen [2]. The AISI 316L austenitic steel with low carbon content (0.030 %) is most often used for biomedical applications. The microstructure of this steel in as-delivered state is mainly austenitic with presence of δ-ferrite in the shape of long stripes and carbides along the grain boundaries, which do not disappear completely even after annealing [4].

In recent years, laser technologies have been increasingly used in the manufacture of medical devices and implants. Laser cutting, laser welding and selective laser melting processes are mainly used [5 - 8]. Because a high-energy source is used and the processes are carried

out by melting and ablation of the metal, changes occur in the microstructure of the laser treated zone, which leads to changes in their properties [9 - 11]. Most of the authors indicate that after laser melting the surface layer consists of a two-phase structure - austenite and δ-ferrite with different morphology depending on the cooling rate [10, 12, 13].

As laser technologies enter more and more intensively in the production of various constructions for medical purposes, it is necessary constantly to conduct research on the microstructure and properties of the materials being processed. Therefore, the aim of the present paper is to investigate the microstructure of laser-melted surface layers of austenitic steel for biomedical applications.

EXPERIMENTAL

Prismatic specimens with dimensions of 10 x 30 x 100 mm^3 were made by milling from AISI 321 (EN X6CrNiTi 18-10) austenitic stainless steel with chemical composition in wt. %: 0.075 % C; 18.20% Cr; 10.85 % Ni; 0.98 Si; 1.82 % Mn; 0.042 % P; 0.012 % S; 0.52 % Ti and Fe the rest. One surface (30 x 100 mm^2) of the sample was ground and treated with a continuous CO_2 laser (initial power N = 1.2 kW and wavelength λ = 10.6 μm). Three modes of laser processing have been selected, which ensure melting of the surface. The treatment mode of sample 1 provides a volume energy density Ev_1 of 31.7 x 10^3 J cm^{-3} and includes: laser beam spot diameter d_1 = 0.4 cm and laser scanning speed V_1 = 0.3 cm s^{-1}. Samples numbered 2 and 3 are processed with Ev_2 = 34.4 x 10^3 and Ev_3 = 28.3 x 10^3 J cm^{-3}, respectively at technological parameters $d_{2,3}$ = 0.3 cm and V_2 = 0.5 and V_3 = 0.6 cm s^{-1}.

To study the microstructure, samples were cut, the cross-section of which was successively grinded with sandpaper with numbers P400, P800, P1200 and P1500. It was then polished sequentially with UltraPad and MetaDi Supreme 9 μm diamond suspension, TriDent and MetaDi Supreme 3 μm diamond suspension and finally with ChemoMet and MasterPrep Aluminum final polishing suspension. The polished surface was etched with solution of HCl:HNO_3 with ratio 3:1.

The microstructure of the austenitic steel and the laser-melted surface layer was investigated with optical microscopes Leica M 80, Olympus SZ51 and XJL-17A and scanning electron microscope Zeiss Evo 10 (Jena, Germany). The micrographs were taken in variable pressure mode using secondary electrons detection. The chemical composition on the surface of the samples was registered with Zeiss SmartEDX energy dispersive X-ray probe.

RESULTS AND DISCUSSION

Microstructure of AISI 321 austenitic steel

The microstructure of the studied steel in as-delivered state is shown in Fig. 1. Grain boundaries and strips of most likely non-metallic inclusions are barely visible on the surface of the polished sample (Fig. 1(a)). It can be seen that after etching the microstructure consists of almost equiaxed austenite grains with different sizes between 20 to 150 μm, a relatively large amount of δ-ferrite in the shape of stripes and spherical carbides along the boundaries of the austenite grains (Fig. 1(d)). Slip lines and twinning are observed in some of the grains. The SEM examination (Fig. 2) confirms that the stripes consist of δ-ferrite rather than non-metallic inclusions. The examination of the chemical composition shows a higher content of chromium in this zone, and a lower content of nickel (Fig. 2(d)). In addition, uneven distribution of the chemical elements in the austenite grains and δ-ferrite is also observed (Fig. 2c). In the austenite grain, the Fe and Cr are of increased content at the boundaries with δ-ferrite. In the δ-ferrite itself, the iron is of lower content, while the chromium is less at the boundaries, rising in the center.

Microstructure of the laser-melted surface layer

The microstructures of the laser-melted surface layers of the studied steel are shown in Fig. 3 and Fig. 4. The boundaries of the laser-melted layer and the absence of a striated structure are noticeable after polishing (Fig. 3(a) and Fig. 4(a)). Different morphology of the base metal and the molten layer is clearly visible after etching. Decreasing the volume energy density from 34.4 x 10^3 J cm^{-3} (sample 2) to 28.3 x 10^3 J cm^{-3} (sample 3) naturally leads to a decrease in the laser-melted layer sizes both in width and in depth (Fig. 3(b) and Fig. 4(b)). Examination at higher _molten zone (MZ), a heat affected zone (HAZ), where melting begins, and

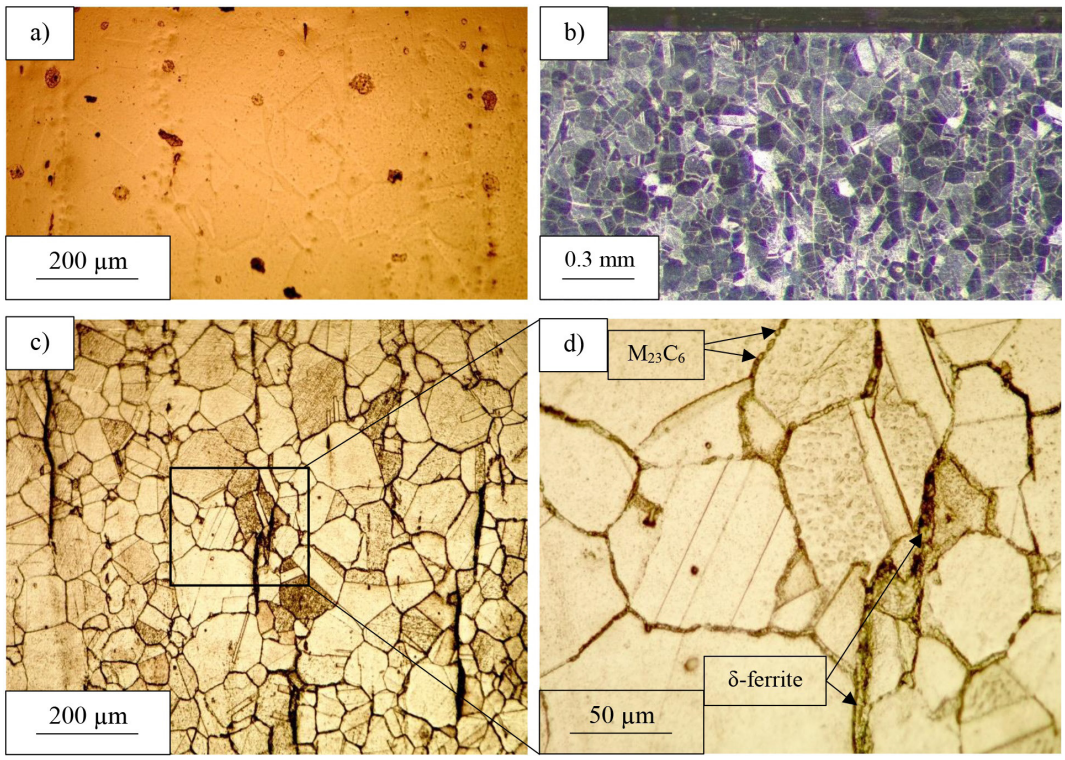

Fig. 1. Microstructure of AISI 321 austenitic steel: a) - after polishing; b), c), d) - after surface etching.

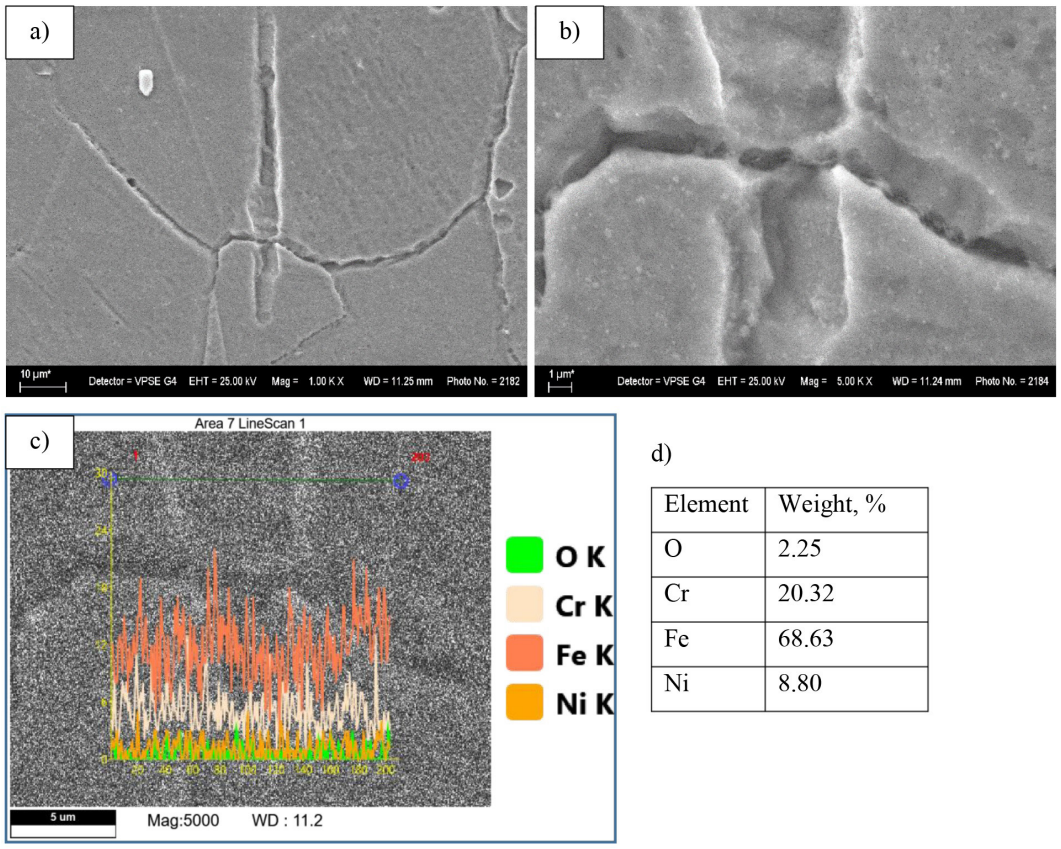

d)

Element	Weight, %
O	2.25
Cr	20.32
Fe	68.63
Ni	8.80

Fig. 2. Delta-ferrite in the microstructure of: a), b) - AISI 321 austenitic steel; c), d).- chemical composition in the zone of δ-ferrite.

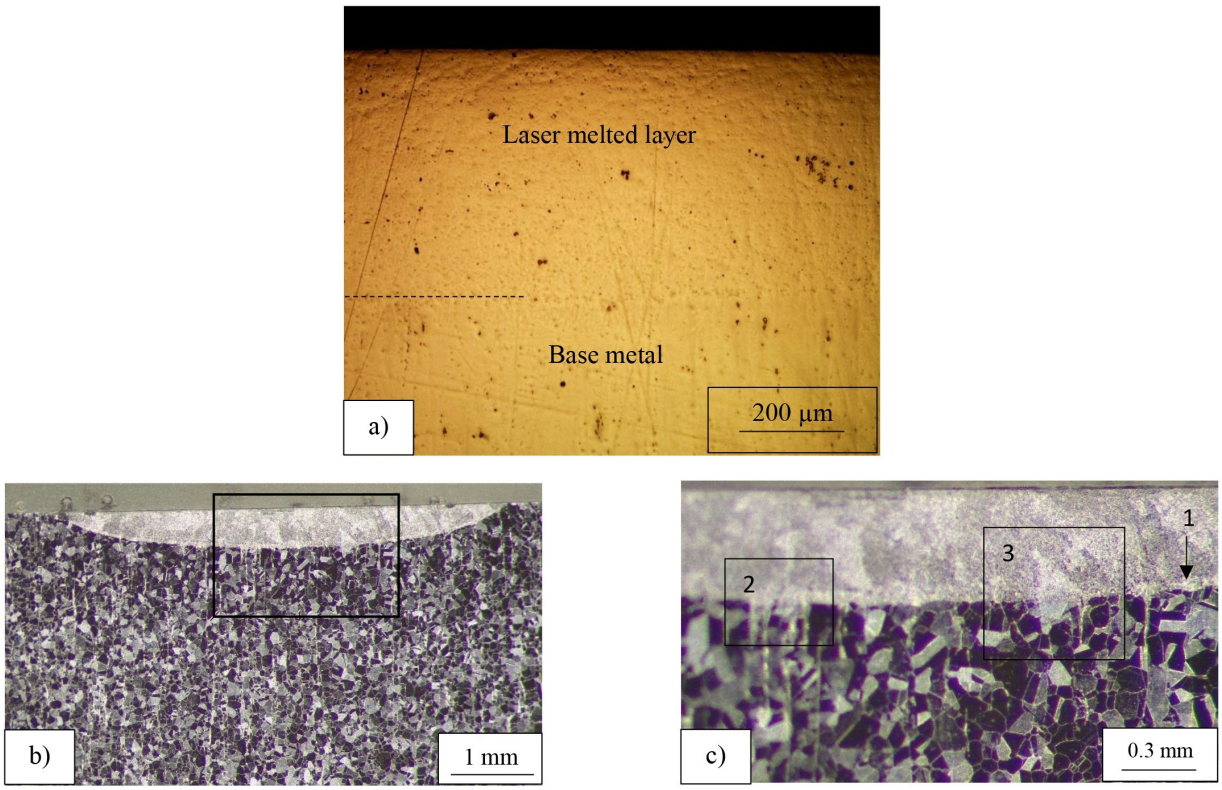

Fig. 3. Microstructure of laser melted surface layer of AISI 321 steel: a) - after polishing; b), c) - after surface etching (sample 2).

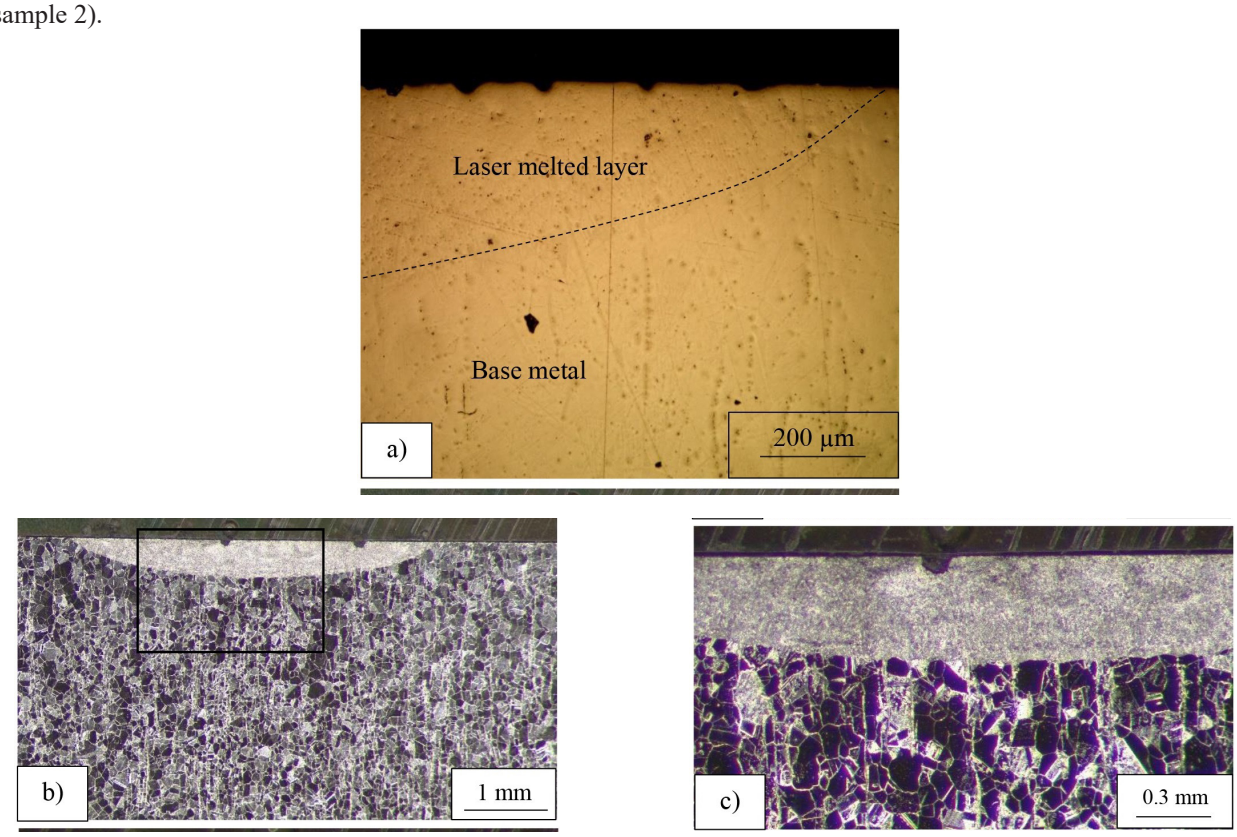

Fig. 4. Microstructure of laser melted surface layer of AISI 321 steel: - a) after polishing; b), c) after surface etching (sample 3).

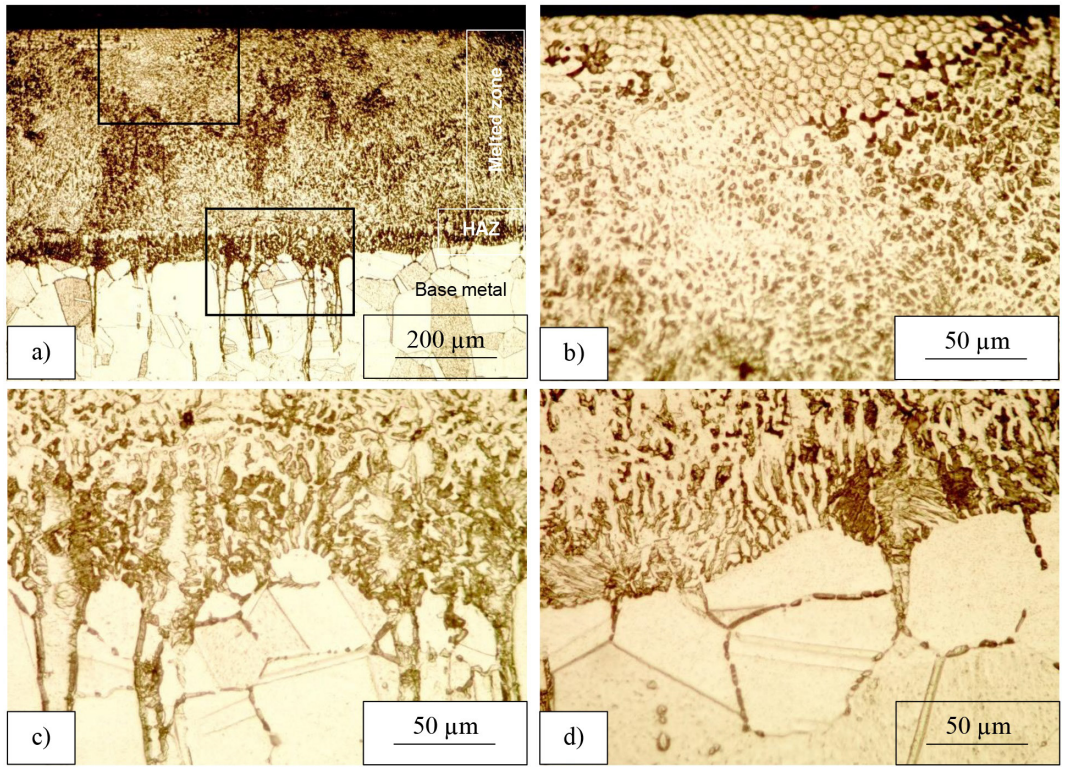

Fig. 5. Microstructure of laser melted : a) - surface layer of AISI 321 steel; b) - top surface; c), d) - boundary between melted layer and base metal.

a base metal (Fig. 5(a)). The MZ is characterized by a dendritic morphology, with a difference in the size and direction of the dendrites in the particular regions. At the top surface, where the melt contacts the air and the cooling rate is highest, fine equiaxed dendrites are observed (Fig. 5(b)). The dendrites at the molten pool bottom and in the HAZ are directed in the heat removal direction. Interestingly, melting occurs more intensively in the δ-ferrite grains (Fig. 5(c)). Structural heredity is also observed in the HAZ along the base metal boundary, where the dendrites grow within the original austenite grain (Fig. 5(d)).

The SEM examination (Fig. 6) confirms the above observations. At high magnifications (Fig. 6(c)), the particular phases can be distinguished - austenite in the dendrites and δ-ferrite in the interdendritic areas. Carbides are not observed. Investigation the chemical composition (Fig. 6(d)) shows a Fe decrease and a Cr increase in the interdendritic areas. In the dendrite itself, the iron has a higher content while chromium has a lower content. It is clearly seen in Fig. 7(a),(b) that the melting starts at the boundaries between the ferrite and austenite grains and proceeds mainly into the ferrite. The pictures in Fig. 7(c),(d) confirm the structural inheritance along the melting boundary.

Results analysis

The present study has shown that the microstructure of as-delivered AISI 321 austenitic steel is relatively inhomogeneous in both morphology and chemical composition. It consists of austenite grains varying in size from 20 to 150 µm, striped δ-ferrite and spherical carbides along the grain boundaries. Due to the presence of Ti and Cr as alloying elements, the carbides are most likely of the $M_{23}C_6$ mixed type [2, 11]. The present microstructure is a result of the production process. In order to achieve a homogeneous microstructure, AISI 321 steel have to be subjected to annealing before fabricating of any types of details.

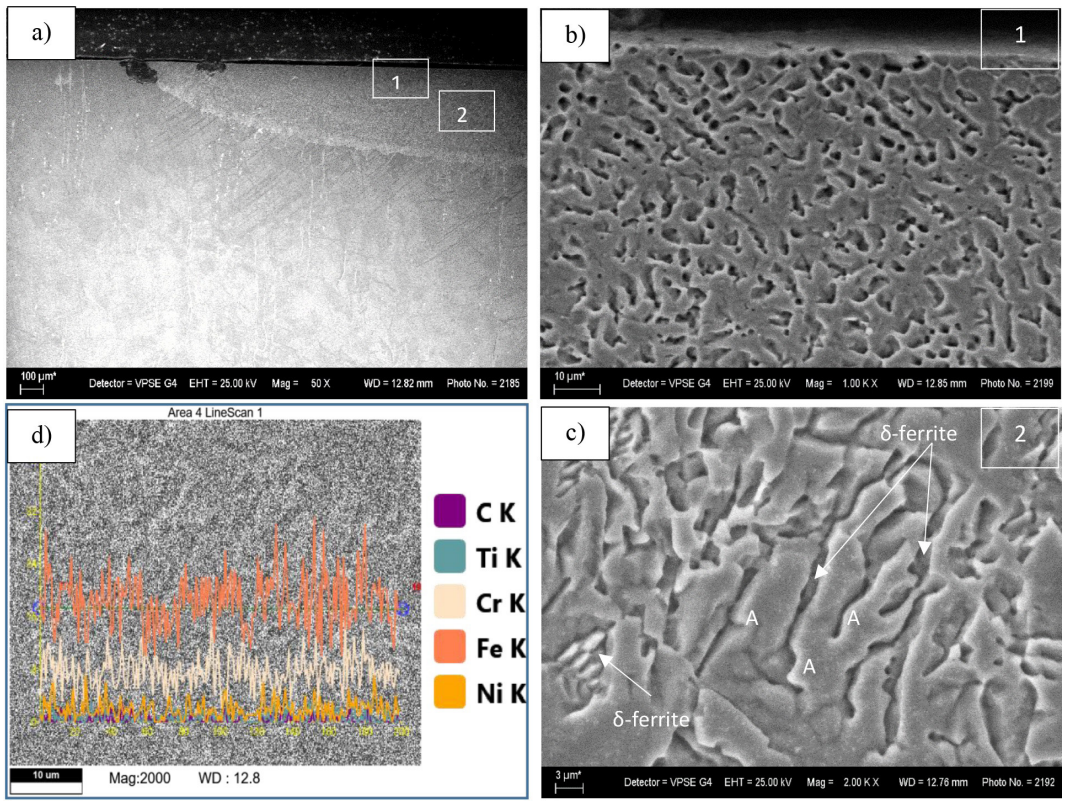

Fig. 6. Microstructure of laser melted surface layer of AISI 321 steel - a), b), c); chemical composition in the melted zone - d). (A - austenite).

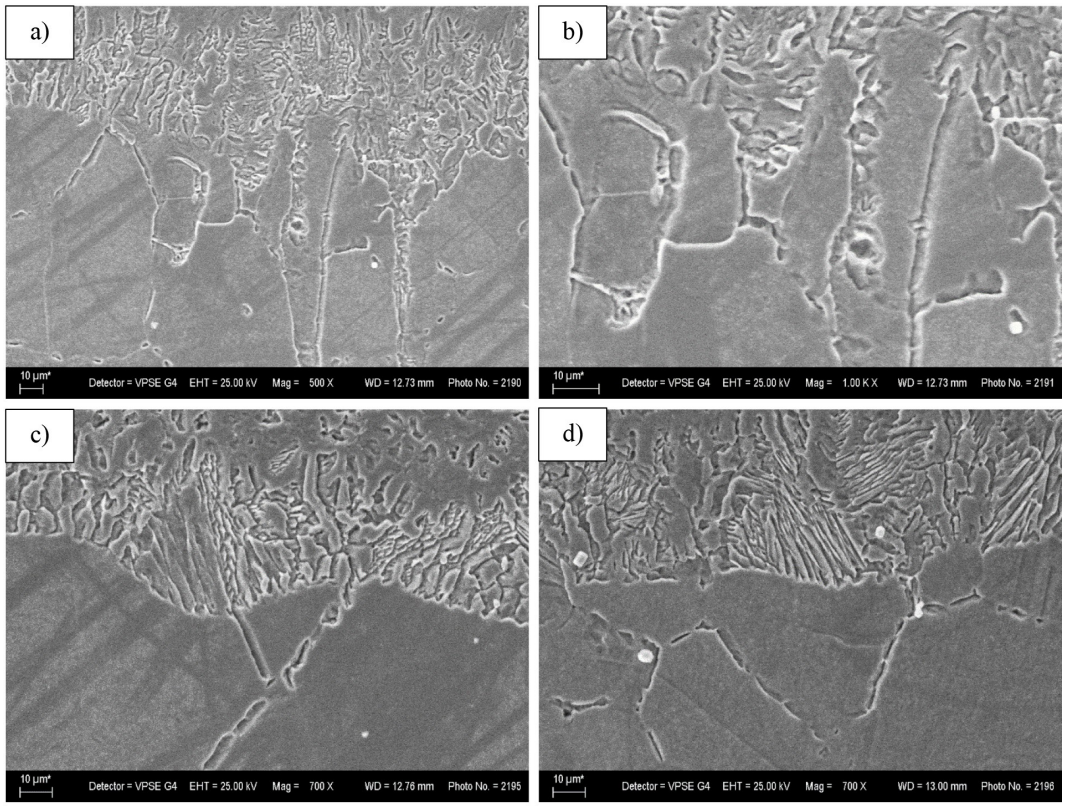

Fig. 7. Microstructure at the boundary layer between melted zone and base metal.

It should be noted that there are still controversies in the study of laser treated austenitic steels. In the work of Stavrev D. et al., the microstructure of AISI 321 steel consists mainly of austenite, and after laser surface treatment, the microstructure is two-phase (δ-ferrite and austenite) in all technological modes used [10]. While in the study of Cui C.Y. et al. AISI 304 steel is characterized by a two-phase structure of α-Fe (ferritic phase) and γ-Fe (austenitic phase) [9]. After melting the surface with a laser, the amount of ferrite phase decreases with increasing the energy density. At the highest value used, α-Fe disappears and the laser-melted layer is characterized only by a single-phase austenite structure.

The microstructure observed in the surface layer of the studied steel after laser melting confirms the results of other scientists [10, 12, 14]. It is more homogeneous compared to the base metal. Carbides and δ-ferrite in the shape of long stripes are not observed. Delta-ferrite is located in the interdendritic areas (Fig. 6(c)). Its amount is greater in the HAZ and there it is characterized with "lathy" morphology (Fig. 5(c),(d) and Fig. 7(c),(d) [10, 12]. Fluctuations in the chemical composition are analogous to those in the structure of the base metal. In the interdendritic areas, the Fe content is lower and the Cr content is higher, which confirms the presence of δ-ferrite (Fig. 6(d)).

CONCLUSIONS

The microstructure of AISI 321 austenitic steel after laser surface melting is investigated in the present paper. It was found that the microstructure before the laser treatment was two-phase and relatively inhomogeneous in morphology and chemical composition. It consists of austenite with a grain size between 20 - 150 μm, relatively large amount of striped δ-ferrite and spherical carbides along the grain boundaries. After laser melting, the microstructure remains two-phase (δ-ferrite and austenite), but becomes more homogeneous in morphology and composition. Different dendrites morphology in the particular regions of the molten layer were confirmed - fine equiaxed dendrites on the top surface and columnar dendrites at the bottom of the molten pool. Delta-ferrite is located in the interdendritic areas and in larger amounts in the transition zone between the molten layer and the base metal.

Acknowledgements

This study is financed by the European Union-NextGenerationEU, through the National Recovery and Resilience Plan of the Republic of Bulgaria, project No BG-RRP-2.004-0009-C02.

REFERENCES

1. M. Kiel, A. Krauze, J. Marciniak, Corrosion resistance of metallic implants used in bone surgery, Arch. Mater. Sci. Eng., 30, 2, 2008, 77-80.
2. Q. Chen, G.A. Thouas, Metallic implant biomaterials, Mater. Sci. Eng.: R: Reports, 87, 2015, 1-57.
3. X. Yan, W. Cao, H. Li, Biomedical alloys and physical surface modifications: a mini-review, Materials, 15, 1, 2021, 66.
4. G.V. Voort, G.M. Lucas, E.P. Manilova, Metallography and microstructures of stainless steels and maraging steels, Metallogr. Microstruct., 9, 2004, 670-700.
5. L. Zhang, Laser welding of dental alloys: a review, J. Mater. Sci.: Materials in Medicine, 2012.
6. C. Bertrand, Y. Le Petitcorps, L. Albingre, V. Dupuis, Prosthodontics: The laser welding technique applied to the non precious dental alloys procedure and results, Br. Dent. J., 190, 5, 2001, 255-257.
7. D.I.C.S. Cosmin, Manufacturing of implants by selective laser melting, Balneo Res. J., 3, 3, 2012, 85-90.
8. L.A. Dobrzański, A. Achtelik-Franczak, M. Król, Computer aided design in Selective Laser Sintering (SLS) - application in medicine, J. Achiev. Mater. Manuf. Eng., 60, 2, 2013, 66-75.
9. C.Y. Cui, X.G. Cui, Y.K. Zhang, Q. Zhao, J.Z. Lu, J.D. Hu, Y.M. Wang, Microstructure and corrosion behavior of the AISI 304 stainless steel after Nd: YAG pulsed laser surface melting, Surf. Coat. Technol., 206, 6, 2011, 1146-54.
10. D. Stavrev, T. Dikova, V. Shtarbakov, M. Milkov, Laser surface melting of austenitic Cr-Ni stainless steel, Adv. Mater. Res., 264, 2011, 1287-92.
11. W.K. Chan, C.T. Kwok, K.H. Lo, Effect of laser surface melting and subsequent re-aging on microstructure and corrosion behavior of aged S32950 duplex stainless steel, Mater. Chem. Phys., 207, 2018, 451-464.
12. D. Baldissin, M. Baricco, L. Battezzati,

Microstructures in rapidly solidified AISI 304 interpreted according to phase selection theory, Mater. Sci. Eng.: A, 449, 2007, 999-1002.
13. R.S. Huang, L. Kang, X. Ma, Microstructure and phase composition of a low-power YAG laser-MAG welded stainless steel joint, J. Mater. Eng. Perform., 17, 2008, 928-35.
14. C.T. Kwok, H.C. Man, F.T. Cheng, Cavitation erosion and pitting corrosion of laser surface melted stainless steels, Surf. Coat. Technol., 99, 3, 1998, 295-304.